Aluminum-Modified Plasma Nitriding with High Efficiency and Enhanced Performances

Ze He , Wei Wei , Jing Hu * , Jingyi Gu *

Posted Date: 20 August 2024

doi: 10.20944/preprints202408.1492.v1

Keywords: aluminum-modified plasma nitriding; effective hardening layer; compound layer; wear behavior; nitriding efficiency

 doi:10.20944/preprints202408.1492.v1

Article

Aluminum-Modified Plasma Nitriding with High Efficiency and Enhanced Performances

Ze He [1], Wei Wei [1,2], Jing Hu [1,2,*] and Jingyi Gu [3,*]

[1] Jiangsu Key Laboratory of Materials Surface Science and Technology, Changzhou University, Changzhou 213164, China
[2] Huaide College, Changzhou University, Jingjiang 214500, China
[3] Restoration Department, Changzhou Stomatological Hospital, Changzhou 213003, China
* Correspondence: jinghoo@126.com (J.H.); gujingyi@126.com (J.G.); Tel.: +86-0519-8633-0095 (J.H.); Tel.: +86-0519-8680-4028 (J.G.)

Abstract: In order to enhance the efficiency and combined performances of nitriding layer, aluminum-modified plasma nitriding (Al-PN) was developed in this research by adding some FeAl particles around the samples during plasma nitriding (PN) for 42CrMo steel. The results show that the efficiency is dramatically enhanced almost 6 times comparing with traditional PN, with the effective hardening layer increasing from 224 μm to 1246 μm at 520℃/4h. More importantly, the compound layer increased just a little bit from 11.64 μm to 14.32 μm, which remarkably reduces the ratio of the compound layer thickness to effective hardening layer thickness, thus being quite beneficial to decrease the brittleness level, making the brittleness level decreasing from Level 4 to Level 1. Meanwhile, ultra-high surface hardness and excellent wear behaviors are obtained by aluminum-modified plasma nitriding (Al-PN) due to the formation of dispersed strengthening phased of AlN and Fe_xAl in the nitriding layer, with the surface hardness increasing from 755 $HV_{0.025}$ to 1251 $HV_{0.025}$, wear rate decreasing from 8.15 $x10^{-5}g{\cdot}N^{-1}{\cdot}m^{-1}$ to 4.07 $x10^{-5}g{\cdot}N^{-1}{\cdot}m^{-1}$. In other words, comparing with PN, the wear resistance has been almost doubled by Al-PN. Therefore, the research can provide comprehensive insights into the surface characteristics and combined performances of the aluminum-modified plasma nitriding layer.

Keywords: aluminum-modified plasma nitriding; effective hardening layer; compound layer; wear behavior; nitriding efficiency

1. Introduction

Plasma nitriding is an environmental friendly surface modification technology, which has been widely used in engineering applications to improve the surface properties of metal components [1–5]. However, plain carbon steel and low alloyed steels are not quite suitable for traditional plasma nitriding in some applications, since too thick compound layer can be formed once the effective hardening layer meets the requirements, which is easy to result in premature failure due to the thicker compound layer' cracking [6–10].

Generally, a nitrided layer is composed of a compound layer on the top surface and a diffusion layer beneath. Since the compound layer has totally different crystal structure from that of the diffusion layer, and thus the two layers are difficult to cooperate with deformation. Therefore, thick compound layer has strong tendency to crack while subjected to heavy impact loads, thus ready to result in premature crack failure [11–15], though a thick effective hardening layer is necessary to enhance the resistance to heavy impact loads.

Because of the above reasons, it is necessary to obtain a plasma nitriding layer with thicker effective hardening layer and thinner compound layer to meet the service requirements in practical applications, especially for components subjected to heavy impact loads. The following two ways are the traditional methods to make a compound layer become thinner: one is adjusting the nitriding parameters, including nitriding temperature, duration, or nitrogen potential to get thinner nitrided

 doi:10.20944/preprints202408.1492.v1

layer [16–20], the other is grinding the very surface layer to reduce the compound layer thickness [21,22]. Unfortunately, the first way is generally accompanied with a thin effectively hardening layer, which brings about lower surface hardness and poorer wear performances, thus hard to meet the long service life requirements of components subjected to heavy impact loads, though premature crack can be avoided [16–20]. And the second way is really hard to control and conduct due to the very high hardness and brittleness of the compound layer.

By comparing the characteristics of nitriding layer obtained at the same nitriding condition for different kind of steels with different amount of alloy elements and similar carbon content, e.g. 45 steel, 42CrMo and H13, it is found that the compound layer is getting thinner, and the effectively hardening layer is getting thicker with the increase of the content of alloying elements [23–27], thus a prediction can be made that adding alloy elements during plasma nitriding may have an effect on thinning the compound layer and thickening the effectively hardening layer.

Since aluminum is the strongest nitride forming element, and it is used as alloying element in the typical nitrided steel of 38CrMoAl to enhance the nitriding performance [28–30]. And it has been found in our previous research that higher nitriding efficiency and better performances can be brought about by depositing aluminum hydroxide film on the surface of samples by electrolyzing aluminum nitrate [31–33]. Unfortunately, the adopted method for introducing aluminum source prior to plasma nitriding is un-environmental friendly and complicated, thus a simple and environmental friendly aluminum-modified plasma nitriding technology was developed by adding FeAl particles around the samples during plasma nitriding process in this research, and the effect of aluminum addition on nitriding efficiency and performances was investigated and compared with those by conventional plasma nitriding for 42CrMo.

2. Materials and methods

Quenched and tempered 42CrMo steel with a hardness of about 320HV was used in this research and its chemical compositions (wt. %) is as below: C: 0.42; Cr: 0.92, Mo: 0.20; Mn: 0.85; Si: 0.30; P: 0.014; S: 0.011; and Fe: balance. Samples with the dimension of 10 mm × 10 mm× 5 mm were machined and ground step by step using different grades of sandpaper, then subjected to ultrasonic cleaning in alcohol for 10 min.

Plasma nitriding was conducted at 520 °C for 4 h in a mixture gas of 25% N_2 + 75% H_2, and with a gas pressure of 400 Pa, followed by furnace cooling. FeAl particles were put around the samples for aluminum-modified plasma nitriding, and traditional plasma nitriding was also conducted as a reference for comparative study. In order to investigate the weight change after different kind of nitriding, the weight of the samples before and after plasma nitriding was weighed by MST-5000 electronic balance, and the weight change was calculated for both cases.

The cross-sectional microstructure was observed by a DMI-3000M optical microscope. The phase compositions were detected by D/max-2500 X-ray diffractometer with Cu-Kα radiation (λ=1.54 Å) under a scanning speed of 1◦/min with a 0.02◦ step size. The surface morphology and micro-regional chemical composition were characterized by a scanning electron microscope (SEM, ZEISS EVO 18) equipped with energy dispersive spectroscopy (EDS). Meanwhile, the 3D surface topography and roughness of the nitrided specimens was characterized by a Laser confocal microscope (DMA8000).

The cross-sectional microhardness was measured by a Vickers hardness tester (HXD-1000TMC) with a load of 25 g and a holding duration of 15 s, each hardness value was determined by averaging at least three measurements to ensure reliable. Meanwhile, according to the Chinese national standard [34], the brittleness level of the nitriding layer was evaluated based on the cracking extent of indentation corners after Vickers hardness test with the load of 500g. The wear behavior was evaluated by a friction and wear tester, GCr15 steel balls were used as the grinding material, with a diameter of 5 mm, the rotation speed of 214 r/min, the loading load of 200 g, and the grinding time of 15 min. The friction coefficient was recorded and the wear tracks were observed using an optical microscope (DMI-3000M), the weight of the samples before and after wear test was weighed by electronic balance (MST-5000), and the wear weight loss was calculated for getting the wear rate. All the wear tests were repeated three times for each case to ensure the reliability of the results.

 doi:10.20944/preprints202408.1492.v1

3. Results and discussion

3.1. Cross-sectional microstructure

Figure 1 presents the cross-sectional microstructure of samples after different PN treatment. It can be seen that after the same nitriding parameter of 520℃/4h, the compound layer thickness is 11.64μm and 14.32μm for conventional plasma nitriding treatment and aluminum-modified plasma nitriding, respectively, which illustrates that the thickness of compound layer increases slightly by aluminum addition under this condition. And it needs to be noted that a compound layer thickness of 5.75μm is obtained by aluminum-modified plasma nitriding at 520℃/0.5h.

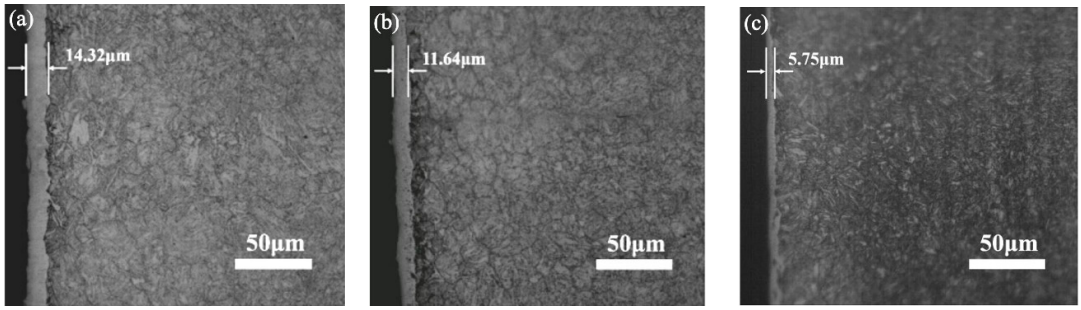

Figure 1. Cross sectional microstructure of samples treated by different PN treatments (a)4h Al-PN, (b) 4h PN, (c) 0.5h Al-PN.

3.2. Surface hardness and effective hardening layer

The cross sectional microhardness profile of samples after different PN treatment is shown in Figure 2. The effective hardening layer thickness is defined as the vertical distance from the very surface to the position with hardness 50 HV higher than that of the substrate hardness [34], and the process efficiency is determined by the effective hardening layer thickness obtained per hour. It can be seen that the surface hardness and effective hardening layer are significantly enhanced by aluminum addition under the same process condition of 520℃/4h. The surface hardness is increased from 755 $HV_{0.05}$ to 1251 $HV_{0.05}$, enhanced by about 500 HV; and the effective hardening layer was dramatically increased from 224 μm to 1246 μm, enhanced by more than 5 times, which illustrates that ultra high process efficiency was obtained by aluminum addition. It needs to be emphasized that a surface hardness of 790 $HV_{0.05}$ and an effective hardening layer of about 435 μm was formed by aluminum-modified plasma nitriding for only 0.5h, which is higher than 755 $HV_{0.05}$, and almost twice of 224 μm formed by traditional plasma nitriding for much longer time of 4h. Combined with the compound layer comparison in Figure 1, it can be concluded that thinner compound layer, thicker effective hardening layer and with higher hardness can be obtained by aluminum-modified plasma nitriding for 42CrMo steel, which is recognized as the ideal characteristics of the nitriding layer for components subjected to heavy impact loads.

 doi:10.20944/preprints202408.1492.v1

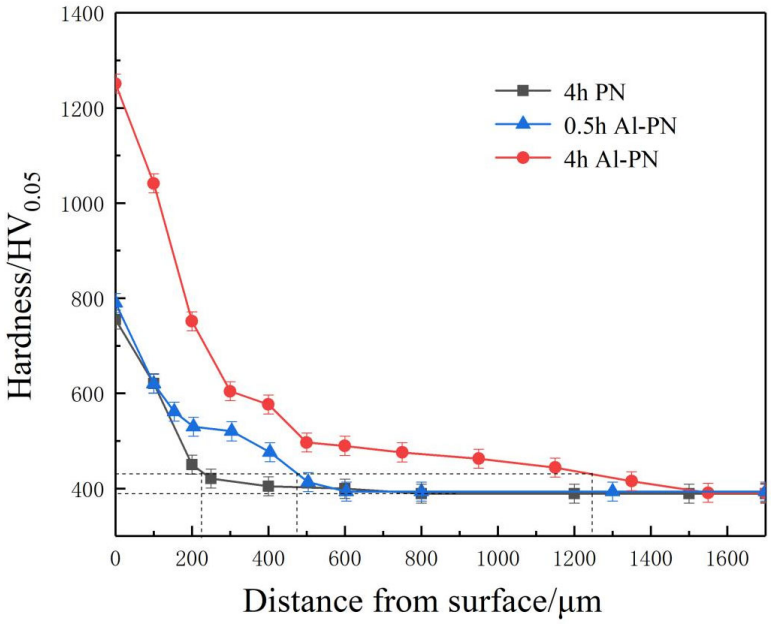

Figure 2. Cross sectional microhardness of samples treated by different PN treatments.

3.3. XRD analysis

X-ray diffraction patterns of samples treated by conventional PN and Al-PN under the same process of 520℃/4h are shown in Figure 3. It can be seen that the patterns corresponding to AlN and Fe_xAl appeared, and the intensity of γ′-Fe_4N and ε-$Fe_{2-3}N$ decreased for the Al-PN treated sample comparing with those of conventional PN treated sample; which illustrates that hard phases of AlN and Fe_xAl were formed during PN treatment due to aluminum addition. And combining the hardness comparison shown in Figure 2, a preliminary conclusion can be drawn that the remarkable increase of hardness of the Al-PN treated layer is mainly attributed to the dispersion strengthening of the hard phases formed in the nitriding layer.

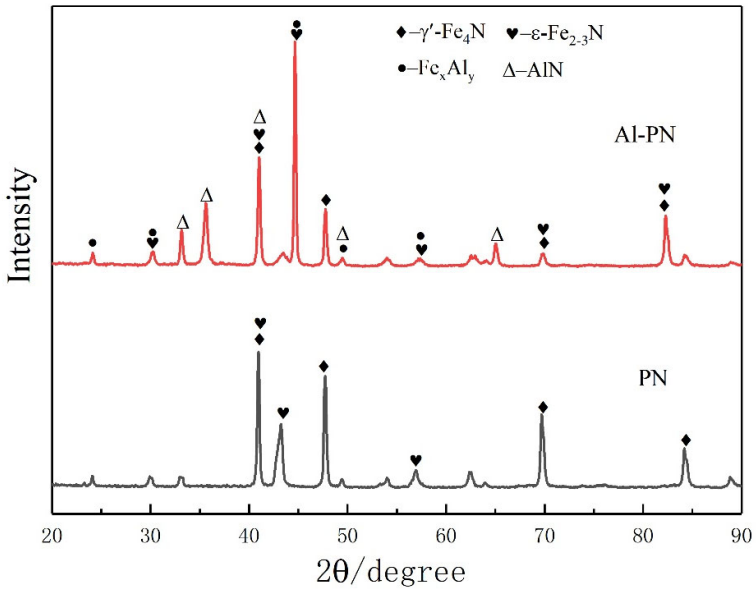

Figure 3. X-ray diffraction patterns of samples treated by PN and Al-PN at 520℃/4h.

 doi:10.20944/preprints202408.1492.v1

3.4. Surface morphology and element analysis

Figure 4 shows the surface morphology of samples by conventional PN and Al-PN under the same process of 520℃/4h, and EDS elements analysis is shown in Table 1. As can be seen that nitride particles were formed and distributed uniformly on the surface, and the EDS element analysis demonstrated there exists 1.64% Al and 3.88% N on the surface of Al-PN treated sample, much higher than that of 1.29% N and without Al for the conventional PN treated sample, which illustrated that Al addition during PN process can not only make Al atoms be sputtered on the surface, but also make much more N atoms absorb on the surface due to the strong affinity of Al and N, thus promote the nitride particles formation and N diffusion inwards, leading to much higher hardness and much thicker effective hardening layer. In other words, much higher nitriding efficiency and better performance can be obtained by Al addition during PN process.

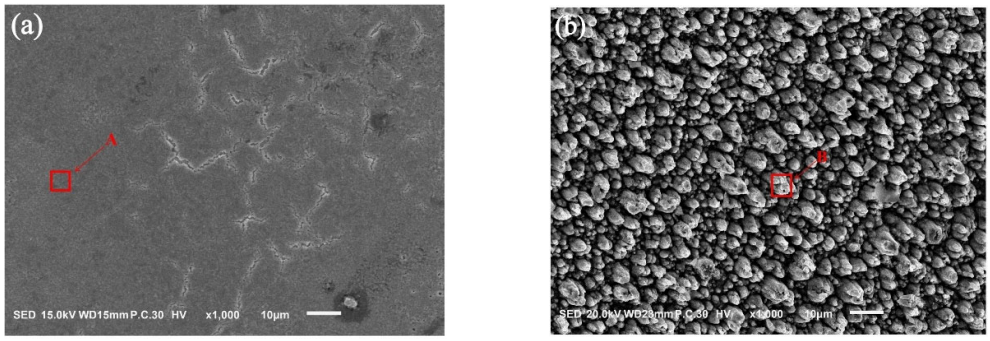

(a) conventional PN, **(b)** Al-PN

Figure 4. Surface morphology of samples nitrided at 520℃/4h.

Table 1. EDS element analysis and weight increase results *(wt/%)*.

Sample	Area	Fe	Al	N
PN	A	98.71	/	1.29
Al-PN	B	94.48	1.64	3.88

3.5. Surface topography and roughness

It has been reported that the surface topography and roughness has significant influence on the wear behavior [30]. Figure 5 presents the 3D surface topography and roughness of samples treated by conventional PN and Al-PN under the same process of 520℃/4h. It determined that the surface roughness Ra of sample Al-PN treated and PN treated is 1.14 μm and 1.08 μm, respectively, i.e. the surface roughness has been decreased by Al addition.

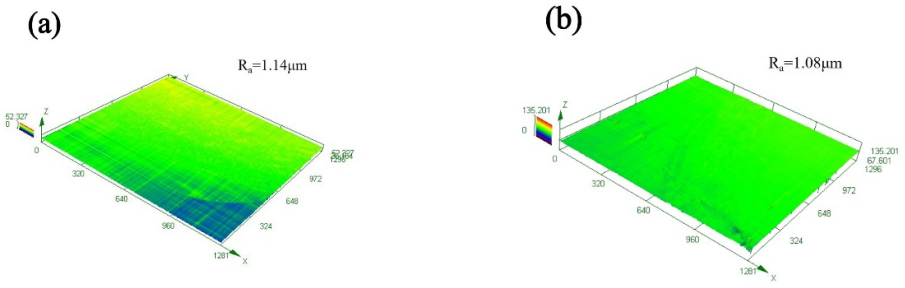

Figure 5. 3D surface topography and roughness of samples nitrided at 520℃/4h(a) conventional PN, (b) Al-PN.

 doi:10.20944/preprints202408.1492.v1

3.6. Wear behaviors

Figure 6 shows the friction coefficient of samples treated by conventional PN and Al-PN under the same process of 520℃/4h. It can be seen that the friction coefficient of sample PN treated and Al-PN treated is 0.75 and 0.64, respectively, i.e. the friction coefficient has been decreased and the friction coefficient curve was more stable for the sample treated by Al-PN, which may be attributed to the corresponding lower surface roughness as shown in Figure 5.

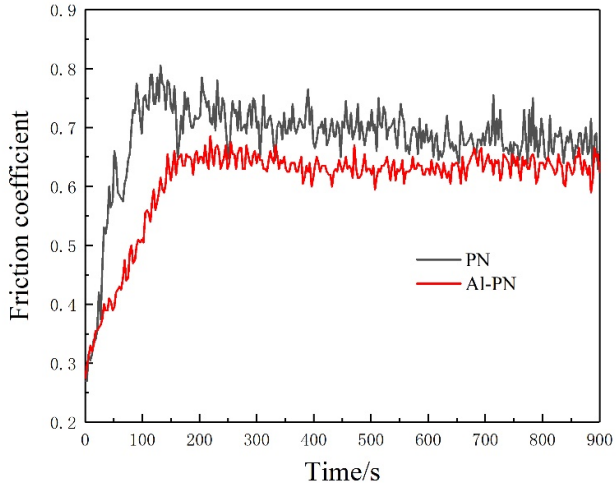

Figure 6. Friction coefficient of samples treated by PN and Al-PN at 520℃/4h.

Wear marks is a visible proof to show the wear extent. Figure 7 shows the wear marks morphologies of samples treated by conventional PN and Al-PN under the same process of 520℃/4h. It demonstrates that the wear marks are much wider and deeper for the sample treated by conventional PN, and with a large amount of grinding grooving and pits on the surface, while the wear marks are much narrower and shallower for the sample treated by Al-PN, and with very few wear pits. By comparing the wear marks, it is clear that the wear resistance is enhanced by Al-PN.

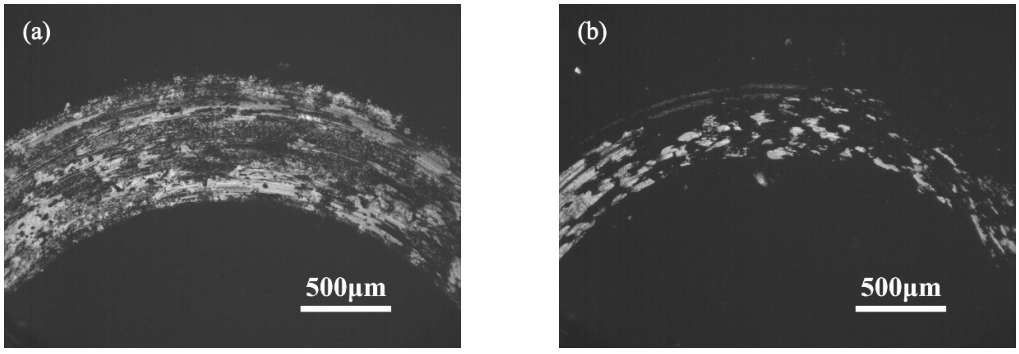

Figure 7. Wear marks morphology of samples treated by PN and Al-PN at 520℃/4h.(a) PN, (b) Al-PN.

In order to make a quantitative comparison of the wear behavior, samples were weighed before and after wear test and the wear rate $\delta = \frac{m_1 - m_2}{N \cdot L}$ was calculated based on the following formula [24] ,

$$\delta = \frac{m_1 - m_2}{N \cdot L} \quad (1)$$

Where, m_1, m_2, N, and L are the weight of the sample before wear test, the weight after wear test, applied load and sliding distance, respectively.

 doi:10.20944/preprints202408.1492.v1

As shown in Figure 8, the wear rate of sample PN treated and Al-PN treated is $8.15x10^{-5}g{\cdot}N^{-1}{\cdot}m^{-1}$ and $4.07x10^{-5}g{\cdot}N^{-1}{\cdot}m^{-1}$, respectively, i.e. the wear rate was reduced by a factor of approximately 2 for the sample treated by Al-PN, which means that the wear resistance was almost doubled by aluminum addition, in good agreement with the increase extent of surface hardness as shown in Figure 2.

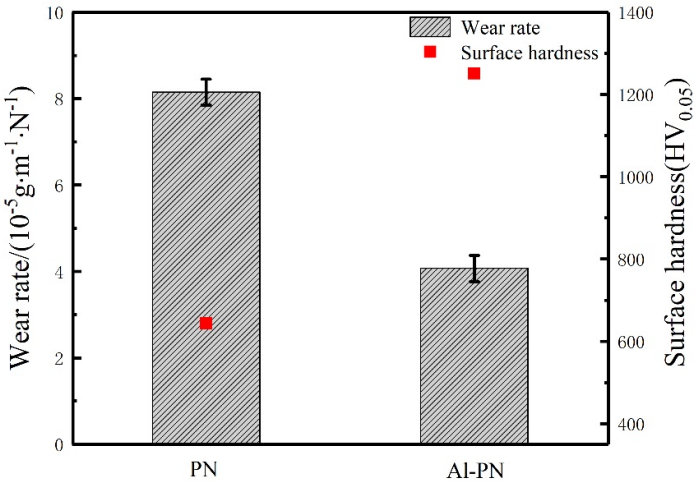

Figure 8. Wear rate of samples treated by PN and Al-PN at 520℃/4h, with surface hardness embedded.

3.7. Brittleness analysis

Brittleness refers to the tendency of a metal to break without being significantly distorted once exposed to a high level of stress, and based on the Chinese national standard[30], the brittleness level of the nitriding layer is divided into 5 Grades according to the cracking extent of the indentation after Vickers hardness test, which are as below: Grade 5 brittleness represents the most brittle, with severe cracking on four sides and/or corners of the indentation; Grade 4 brittleness corresponds to cracking on three sides and/or corners; Grade 3 brittleness corresponds to cracking on two sides and/or corners; Grade 2 brittleness corresponds to cracking on one side and/or corner; and Grade 1 brittleness means the least brittle, corresponding to no cracking around all the indentation, and thus represents the best toughness. Generally, Grade 1 brittleness is needed for components subjecting to heavy impact loads in order to have long service life.

The indentations of samples treated by conventional PN and Al-PN under the same process of 520℃/4h are shown in Figure 9. It can be seen that there exists severe cracking on three sides and corners around the indentation of the PN treated sample, so the brittleness is determined to be Grade 4 [34]; while there is no cracking around the indentation of the Al-PN treated sample, thus the brittleness is determined to be Grade 1 [34]. Therefore, a conclusion can be drawn that the brittleness grade can be effectively decreased by aluminum addition, in other words, the toughness can be effectively improved, and the strict technical requirements of the components with both excellent wear resistance and toughness can be met.

Meanwhile, it can be seen that the indentation area of the Al-PN treated sample is much smaller than that of the PN treated sample, which also implies that the surface hardness is enhanced significantly by aluminum addition, being consistent with the results shown in Figure 2 and 8.

 doi:10.20944/preprints202408.1492.v1

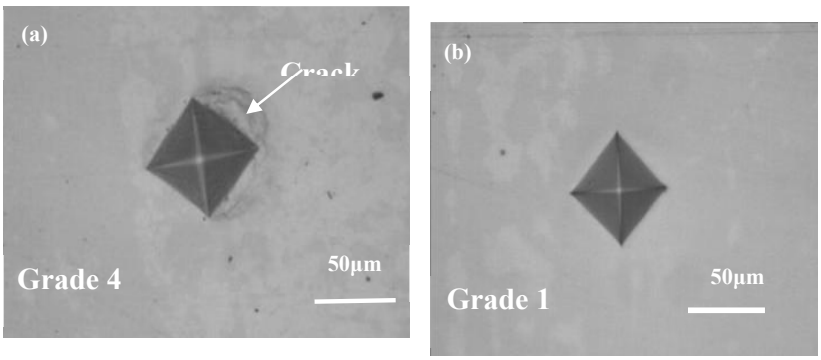

Figure 9. The indentations of samples treated by PN and Al-PN at 520℃/4h. (a) PN, (b) Al-PN.

4. Mechanism and discussions

In order to provide a comprehensive understanding on the amazing effect of aluminum addition on plasma nitriding, the main characteristics and performances of the nitriding layer treated by conventional PN and Al-PN are summarized and compared in Table 2. It can be seen that the surface hardness and effective hardening layer (corresponding to nitriding efficiency) can be dramatically enhanced by Al addition. More valuably, both the wear resistance and toughness are greatly enhanced by Al-PN due to the much higher hardness and much lower ratio of compound layer thickness to effective hardening layer thickness.

Table 2. Comparison of nitriding layer characteristics and comprehensive performances of samples Al-PN and PN treated at 520℃/4h.

Process	Compound layer thickness (μm)	Effective hardening layer thickness (μm)	ratio of compound layer to effective hardening layer	Surface hardness ($HV_{0.05}$)	Wear rate ($10^{-5}g \cdot N^{-1} \cdot m^{-1}$)	Brittleness Level	Phase constituents
PN	11.64	224	0.052	644	8.15	4	$Fe_{2-3}N$, Fe_4N
Al-PN	14.32	1246	0.011	1251	4.07	1	$Fe_{2-3}N$, Fe_4N, AlN, Fe_xAl

Note: the nitriding efficiency is calculated based on the effective hardening layer formed per hour.

The possible mechanism for the above amazing effect of Al addition on the nitriding efficiency and performances can be expressed as follows:

During the plasma nitriding process, ionization has been happened in the thin gas atmosphere resulted from the influence of the high-voltage DC electric field, forming a plasma region composed of N^+, H^+, e^- and N, H active atoms, where N^+ and H^+ ions bombard towards cathode at very high speed under a strong electric field in the plasma region. High-velocity bombardment makes Fe and Al ions splash out to the plasma region.

Due to the strong affinity between Al and N, much more N atoms were absorbed on the surface as confirmed by EDS in Table 1. On one hand, much higher content of N has strong tendency to react with Al to form micro particles of AlN with very high hardness, on the other hand, much higher N gradient can dramatically increase the diffusion rate of nitrogen atoms, thus brings about much longer diffusion distance and stronger solution strengthening effect. Meanwhile, part of active Al atoms can also react with Fe to form FeAl can be formed as well, thus the strong dispersion strengthening effect of AlN and FeAl brings out significant enhancement of hardness in the nitriding layer. Therefore, both the surface hardness and effective hardening layer can be dramatically

 doi:10.20944/preprints202408.1492.v1

enhanced due to the dispersion strengthening and stronger solution hardening resulted from the effect of Al addition, which brings about excellent wear behavior.

Meanwhile, the brittleness level is greatly decreased due to the obvious decrease of the ratio of compound layer thickness to effective hardening layer thickness, in other words, the toughness of the nitriding layer is greatly enhanced, which is of significant value for the components subjected to heavy impact loads.

5. Conclusions

Al-modified plasma nitriding was primarily developed by adding some FeAl particles around the samples during plasma nitriding treatment, and the amazing effect of aluminum addition on both process efficiency and related properties was investigated for 42CrMo steel. The following main conclusions can be drawn comparing with conventional plasma nitriding at the same parameters of 520℃/4h:

- (1) The nitriding efficiency can be dramatically improved by more than 5 times, with the effective hardening layer enhancing from 224 μm to 1246 μm under the same process condition of 520℃/4h. And the surface hardness is higher and effective hardening layer is much thicker for sample treated by Al-PN for only 0.5h than that treated by traditional PN for as long as 4h.
- (2) The surface hardness and wear resistance can be significantly improved, with the surface hardness increasing from 755 $HV_{0.05}$ to 1251 $HV_{0.05}$ and the wear rate reducing from 8.15 $x10^{-5}g{\cdot}N^{-1}{\cdot}m^{-1}$ to 4.07 $x10^{-5}g{\cdot}N^{-1}{\cdot}m^{-1}$, i.e. the wear resistance has been almost doubled.
- (3) The brittleness grade can be greatly decreased by Al-PN under the same process condition due to the much lower ratio of compound layer thickness to effective hardening layer thickness, in other words, the toughness can be effectively improved.
- (4) The developed novel Al-PN can dramatically enhance the production efficiency and save energy for obtaining any required layer thickness, meanwhile, improve service life of the treated components due to owning much better performances.

Author Contributions: Ze He: Conceptualization, Methodology, Experiments, Writing- Original draft preparation. Wei Wei: Investigation, Experiments helper. Jing Hu: Supervisor, Writing- Reviewing and Editing. Jingyi Gu: Visualization, Investigation, Software, Validation, Second Supervisor.

Acknowledgments: This work was supported by National Natural Science Foundation of China (21978025), PAPD & TAPP and Postgraduate Research & Practice Innovation Program of Jiangsu Province (SJCX24_1580).

References

1. Liu, R. L.; Yan, F. Y.; Yan, M. F. Surface grain nanocrystallization of Fe-Cr-Ni alloy steel by plasma thermochemical treatment. Surf. Coat. Tech. 2019, 370, 136-143.
2. Li, J.; Hong, H.H.; Sun, L.; et al. Argon ion sputtering bridging plasma nitriding and GLC film deposition: Effects on the mechanical and tribological properties. Surf. Coat. Tech. 2024, 479,130559.
3. Ni, J.; Ma, H.; Wei, W.; et al. Novel Effect of Post-Oxidation on the Comprehensive Performance of Plasma Nitriding Layer. Coatings, 2024, 14, 86.
4. Hong, H. H.; Xie, G. R.; Sun, L.; et al. The diffusion behavior and surface properties of catalytic nitriding with LaFeO3 film prepared by the sol-gel method. Surf. Coat. Tech. 2023, 467, 129720.
5. Lu, J.S.; Li, B.K. Discussion of precision heat treatment and anti-fatigue manufacturing of gear. J. Mech. Eng. 2019, 43, 170-175.
6. Li, J.; Tao, X.; Wu, W.P.; et al. Effect of arc current on the microstructure, tribological and corrosion performances of AISI 420 martensitic stainless steel treated by arc discharge plasma nitriding. J. Mater. Sci. 2023, 58, 2294-2309.
7. Wang, B.; Liu, B.; Zhang, X.D.; et al. Enhancing heavy load wear resistance of AISI 4140 steel through the formation of a severely deformed compound-free nitrided surface layer. Surf. Coat. Tech. 2018, 356, 89-95.
8. Shen, J.H.; Hu, J.; An, X.L. Regulation of phase partition and wear resistance for FeCoCrV high entropy alloy by heat treatment. Intermetallics. 2024,167: 108232
9. Wang, Z.Y.; Xing, Z.G.; Wang, H.D.; et al. Research status of test method for bending fatigue life of heavy duty gear. Mater. Rev. 2018, 32, 3051-3059.

 doi:10.20944/preprints202408.1492.v1

10. Samal, S.; Cibulková, J.; Ctvrtlík, R.; et al. Tribological Behavior of NiTi Alloy Produced by Spark Plasma Sintering Method. Coatings. 2021, 11, 10.
11. Peng, T. T.; Zhao, X. B.; Hu, J.; et al. Improvement of stamping performance of H13 steel by compound-layer free plasma nitriding. Surf. Eng. 2020, 36, 492-497.
12. Li, J. C.; Yang, X. M.; Wang, S. K.; et al. A rapid D.C. plasma nitriding technology catalyzed by preoxidation for AISI4140 steel. Mater. Lett. 2014, 116, 199-202.
13. Miao, B.; Song, L.; Chai, Y. T.; et al. The effect of sand blasting pretreatment on plasma nitriding. Vacuum. 2017, 136, 46-50.
14. Liu, H.; Li, J. C.; Chai, Y. T.; et al. A novel plasma oxynitriding by using plain air for AISI 1045 steel. Vacuum. 2015, 121, 18-21.
15. Li, L. Z.; Liu, R. L.; Liu, Q. L.; et al. Effects of Initial Microstructure on the Low-Temperature Plasma Nitriding of Ferritic Stainless Steel. Coatings. 2022, 12, 1404.
16. Peng, T.T.; Chen, Y.; Wu, M.H.; et al. Phase constitution control of plasma nitrided layer and its effect on wear behavior under different loads. Surf. Coat. Techno. 2020,403:126403
17. Lu, Y. Y.; Li, D.; Ma, H.; et al. Enhanced plasma nitriding efficiency and properties by severe plastic deformation pretreatment for 316L austenitic stainless steel. J. Mater. Res. Technol. 2021, 15, 1742-1746.
18. Yan, M. F.; Chen, B. F.; Li, B. Microstructure and mechanical properties from an attractive combination of plasma nitriding and secondary hardening of M50 steel. Appl. Surf. Sci. 2018, 455, 1-7.
19. Kim, Y. M.; Son, S. W.; Lee, W. B. Thermodynamic and kinetic analysis of formation of compound layer during gas nitriding of AISI1018 carbon steel. Met. Mater. Int. 2018, 24, 180-186.
20. Saeed, A.; Khan, A. W.; Jan, F.; et al. Optimization study of pulsed DC nitrogen-hydrogen plasma in the presence of an active screen cage. Plasma. Sci. Technol. 2014, 16, 460-464.
21. Ma, H.; Wei, K. X.; Zhao, X. B.; et al. Performance enhancement by novel plasma boron-nitriding for 42CrMo4 steel. Mater. Lett. 2021, 304, 130709.
22. Nishimoto, A.; Nagatsuka, K.; Narita, R.; et al. Effect of the distance between screen and sample on active screen plasma nitriding properties. Surf. Coat. Tech. 2010, 205, S365-S368.
23. Naeem, M.; Torres, A.V.R.; Serra, P.L.C.; et al. Combined plasma treatment of AISI-1045 steel by hastelloy deposition and plasma nitriding. J. Build. Eng. 2022, 47: 103882.
24. Wu, J. Q.; Mao, C. J.; Hu, J.; et al. Titanium-modified plasma nitriding layer and enhanced properties for 42CrMo steel. J. Mater. Res. Technol. 2022, 18, 3819-3825.
25. Gonzalez-Moran, A.K.; Naeem, M.; Hdz-García, H.M.; et al. Improved mechanical and wear properties of H13 tool steel by nitrogen-expanded martensite using current-controlled plasma nitriding. J. Mater. Res. Technol. 2023, 25: 4139-4153.
26. Tang, L.; Jia, W. J.; Hu, J.; et al. An enhanced rapid plasma nitriding by laser shock peening. Mater. Lett. 2018, 231, 91-93.
27. Shen, H. Y.; Wang, L. Oxide layer formed on AISI 5140 steel by plasma nitriding and post-oxidation in a mixture of air and ammonia. J. Alloy. Compd. 2019, 806, 1517-1521.
28. Koutná, N. ; Löfler, L. ; Holec, D. ; et al. Atomistic mechanisms underlying plasticity and crack growth in ceramics: a case study of AlN/TiN superlattices. Acta Mater. 2022, 229: 117809.
29. Sun, J.Q.; Wang, D.R.; Yang, J.; et al. In Situ Preparation of Nano-Cu/ Microalloyed Gradient Coating with Improved Antifriction Properties. Coatings. 2022, 12, 1336.
30. Chen, H.; Wang, W.; Le, K.; et al. Effects of substrate roughness on the tribological properties of duplex plasma nitrided and MoS2 coated Ti6Al4V alloy. Tribol. Int. 2024, 191: 109123.
31. Kang, Q.F.; Wei, K.X.; Fan, H.M.; et al. Ultra-high efficient novel plasma aluminum-nitriding methodology and performances analysis. Scr. Mater. 2022, 220: 114902
32. Zhuang, H.Y.; Kang, Q.F.; Xie, Y.X.; et al. Kinetics analysis and enhancement mechanism of aluminum-enhanced plasma nitriding for 42CrMo steel. J. Mater. Res. Technol. 2023, 24（5）：6588-6594
33. Kang, Q.F.; Fan, H.M.; Yang, X.H.; et al. Evolution of aluminum hydroxide film during plasma nitriding and its enhancement effect. Mater. Lett. 2023, 330: 133348
34. Standardization Administration of China, National standard of the people's republic of China GB/T 11354-2005, Determination of nitrided case depth and metallographic microstructure examination for steel and iron parts.

 doi:10.20944/preprints202408.1492.v1

disclaim responsibility for any injury to people or property resulting from any ideas, methods, instructions or products referred to in the content.